Journal of Applied Electrochemistry **33**: 939–949, 2003.

Development of an integrated process for electrochemical reaction and chromatographic SMB-separation☆

M. MICHEL[1], H. SCHMIDT-TRAUB[1,*], R. DITZ[2], M. SCHULTE[2], JOACHIM KINKEL[3], WALTER STARK[3], MICHAEL KÜPPER[4] and MATTHIAS VORBRODT[5]
[1]*Department of Bio- and Chemical Engineering, University of Dortmund, 44221 Dortmund, Germany*
[2]*Merck KGaA, SLP/New businesses, 64293 Darmstadt, Germany*
[3]*Georg-Simon-Ohm Fachhochschule Nürnberg, 90489 Nürnberg, Germany*
[4]*Institut für Mikrotechnik Mainz, 55129 Mainz, Germany*
[5]*Chemisches Laboratorium Dr. Vorbrodt, 06466 Gatersleben, Germany*
*(*author for correspondence, fax: +49-231-755-2341, e-mail: schmtr@bci.uni-dortmund.de)*

Received 13 November 2002; accepted in revised form 4 July 2003

Key words: arabinose, electrochemical microreactor, process integration, reactive separation, SMB-reactor

Abstract

A new continuous process combining electrochemical reaction and chromatographic simulated-moving-bed (SMB) separation is presented. To demonstrate the potential of process integration, this reactor concept is applied to the direct electrochemical production of arabinose by means of simulation. Experimentally verified models of 'reactor' and 'column' units are combined with a model of the electrochemical SMB-reactor. These process units are characterized individually and their model parameters are discussed. The electrochemical reaction inside the microreactor can be described by a series reaction, which has an impact on the design of the integrated process: as the reaction should take place in areas of the SMB-process with maximum educt concentration, the reactors are switched 'on' and 'off' during operation. The integrated process shows interaction between the reaction and the separation to diminish side reactions. Case studies prove the theoretical feasibility of the integrated process. Compared to a conventional process with a reactor followed by a SMB-separation, higher yields can be obtained.

List of symbols

Latin letters

A_C	cross section of chromatographic column (cm^2)
A_e	electrode surface area (cm^2)
a_e	electrode surface to volume ratio (cm^{-1})
b	width of reactor channel (μm)
Bo	Bodenstein number (–)
c_j	fluid phase concentration of component j (mmol cm^{-3})
Con_j	conversion of component j (–)
$c_{p,j}$	fluid phase concentration in the particle pores of component j (mmol/cm^3)
D_{ax}	axial dispersion coefficient in the reactor ($cm^2\ s^{-1}$)
$D_{ax,C}$	axial dispersion coefficient in the column ($cm^2\ s^{-1}$)
d_p	particle diameter (cm)
F	Faraday constant (9.64846×10^4 C mol^{-1})
H_j	Henry coefficient of component j (–)
i	applied current density (mA cm^{-2})
k_m	rate constant of reaction m (s^{-1})
$k_{eff,j}$	overall mass transfer coefficient of component j (cm s^{-1})
L	reactor channel length (cm)
L_c	column length in the SMB-process (cm)
m_k	dimensionless flow rate in section k (–)
N	number of reactor channels per compartment (–)
n_C	number of columns in the SMB-process (–)
n_e	number of electrons (–)
$\dot{n}_j$	mole flow of component j (mmol $cm^{-3}\ s^{-1}$)
n_R	number of active reactors (–)
Pr_j	productivity of component j (mmol $cm^{-3}\ s^{-1}$)
Pur_j	purity of component j (mmol $cm^{-3}\ s^{-1}$)
q_j	concentration of component j in the stationary phase (mmol $cm^{-3}\ s^{-1}$)
R_j	reaction term for component j (mmol $cm^{-3}\ s^{-1}$)
Re_p	particle Reynolds number (–)
s	distance electrode/membrane (μm)
s_m	membrane thickness (μm)
t	time (s)
t_{switch}	time between switching of the ports in the SMB-process (s)
u	internal fluid velocity in the reactor (cm s^{-1})

☆ This paper was originally presented at the 6th European Symposium on Electrochemical Engineering, Düsseldorf, Germany, September 2002.

V_A volume anode compartment (μl)
$\dot{V}$ flow rate (cm^3 s^{-1})
$\dot{V}_k$ flow rate in section k (cm^3 s^{-1})
x axial coordinate in the column (cm)
Y_j yield of component j (–)
z axial coordinate in the reactor (cm)

Greek letters

ε void fraction (–)
η_{fluid} fluid viscosity (g cm^{-1} s^{-1})
ρ_{fluid} fluid density (g cm^{-3})
τ residence time (s)

Subscripts

0 reactor inlet
I,II,III,IV sections of the TMB and SMB-process
Ara arabinose
D desorbent
E extract
Ery erythrose
F feed
Gluc gluconate
fluid fluid
j component j
k section k
R raffinate
Rm electrochemical reaction number m
S Solid

1. Introduction

The economic production of high-value fine chemicals and pharmaceutical agents requires reactions with high yield and purity. In comparison to the common process design of reaction and separation in series, the integration of both steps in one unit may enhance process performance [1]. The interaction between reaction and separation can increase the reaction yield by continuous removal of products from the reaction zone while simultaneously purifying the products. However, this requires matching operating conditions of the separation and the reaction. This generally leads to a loss of one degree of freedom in process operation and optimization.

The combination of electrochemistry and chromatography for electroorganic synthesis promises to be an interesting application, because both processes operate at moderate conditions concerning temperature, pressure and solvents. As electrochemical reactions are controlled by the applied electric current, the reactors can be switched 'on' and 'off'. This offers an additional operating and design parameter.

In the pharmaceutical industry, preparative chromatography is an established high purity separation process. As the separation factors of these products are rather low, it is difficult or impossible to separate them by other thermal processes. Batch chromatography is a standard process, but in recent years the simulated-moving-bed(SMB)-technology has been established as a continuous process for the purification of pharmaceuticals and fine chemicals [2, 3].

The combination of chromatography with chemical and biochemical reactions in chromatographic reactors is a known process [4]. The application in gas and liquid phases include analytical purposes such as determination of reaction kinetics as well as preparative production of chemicals. A good overview of this topic is provided [5–7].

To implement electrochemical reactions in the SMB-process, microreactors are well suited because of their compact and modular design. Additionally, the characteristic properties of microreactors such as high mass and heat transfer, high surface to volume ratio and small residence times are favourable for process stability and performance [8–10].

To demonstrate the potential of process integration, a new continuous process, the electrochemical SMB-reactor, is discussed. A possible mode of operation of such a SMB-reactor and its theoretical application to the direct electrochemical production of arabinose are examined. Based on the models for the electrochemical microreactor and the chromatographic column, process simulation and case studies are used to get an insight into the behaviour and performance of the integrated process.

2. Chromatographic separation process

2.1. *Batch chromatography*

Batch chromatography is an adsorptive separation process. It is a well known method for the analytical separation of different substances. Another application is the preparation of high purity and high value products in liquid systems. For the separation of two substances A and B, the principle mode of operation is shown in Figure 1.

A mixture of the components A and B is injected as a sharp pulse and is transported through the column by means of a solvent (desorbent). While passing through the column, the two solutes are separated from each other because of different adsorption to the solid phase (adsorbent). The more strongly adsorbed component B has a slower propagation velocity inside the column than component A and leaves the column last.

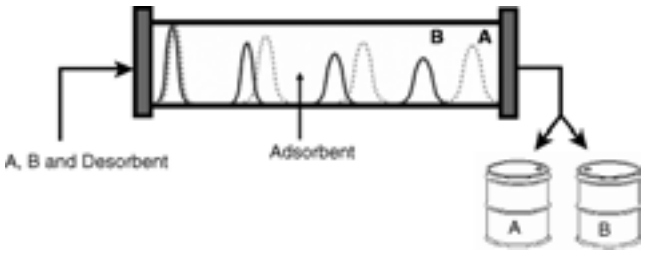

Fig. 1. Operating principle of batch chromatography with concentration profiles at different times.

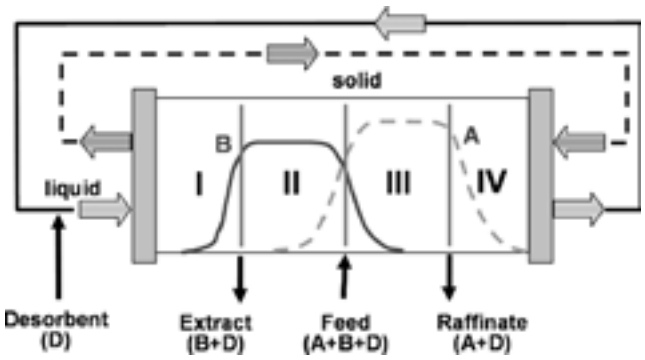

Fig. 2. Operating principle of the TMB-process with internal concentration profiles (steady state).

2.2. *True-moving-bed(TMB)-chromatography*

To improve separation efficiency and to minimize fluid consumption as well as product dilution, the concept of a continuous counter-current flow of the solid and fluid phase was developed. This so called TMB-process separates the feed mixture into two fractions: the raffinate and the extract. The process can be divided into four sections, each of which accomplishes a special task realized by the right choice of flow rates (Figure 2).

The feed is injected between the zone II and III, in which the separation of the two components takes place. According to their adsorption strength, the net transport velocity of components A and B are in the direction of the fluid or the solid, respectively. Therefore the less retarded component A can be collected at the raffinate port at the end of section III and component B at the extract port at the beginning of section II. To ensure a continuous countercurrent process, the solid and the fluid phase have to be cleaned in the sections I and IV respectively. Additional desorbent is injected to clean the solid phase and the purified phases can be recycled.

The process is mainly characterized by the dimensionless flow rates m_k in each section k [11–13]

$$m_k = \frac{\dot{V}_{k,\mathrm{TMB}}}{\dot{V}_\mathrm{S}} \tag{1}$$

In the ideal case without dispersion, mass transfer resistance etc. these dimensionless flow rates can be used to find optimal process conditions depending on the adsorption equilibrium.

The flow rate of the solid $\dot{V}_\mathrm{S}$ is constant throughout the apparatus, but the liquid flow rate $\dot{V}_{k,\mathrm{TMB}}$ changes in each section because of different inlet and outlet flows of feed, desorbent, raffinate and extract.

In practice the movement of the particles is difficult to realize. One reason is the unavoidable backmixing of the solid that reduces the efficiency of the process. Another problem is the abrasion of the particles caused by their movement.

2.3. *Simulated-moving-bed(SMB)-chromatography*

The SMB-process overcomes the difficulties related to the movement of the solid [14]. A countercurrent movement of the solid phase is simulated by moving the fixed beds periodically in the opposite direction to the liquid flow. This is achieved by switching the ports of the inlet and outlet streams in the direction to the liquid flow. The resulting periodic process is at cyclic steady state (Figure 3).

The performance of a SMB unit becomes identical to the corresponding TMB-process in the case of an infinite number of columns and the switching time as well as the column length approaching zero.

The SMB-process has been used for many years in the petroleum and sugar industry for large scale operation [11, 14–17]. In recent years this process has been established in the pharmaceutical industry for the production of pharmaceuticals and fine chemicals with high purity. These applications have been reviewed [3].

3. The electrochemical microreactor

The integrated process employs electrochemical microreactors. A prototype of this reactor is described in [8] and its functionality has already been proven [9]. The

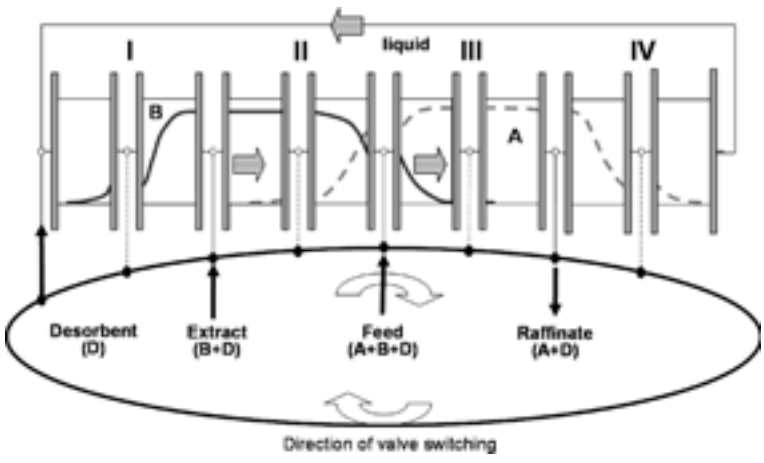

Fig. 3. Operating principle of the SMB-process with internal concentration profiles at the end of one cycle (cyclic steady state).

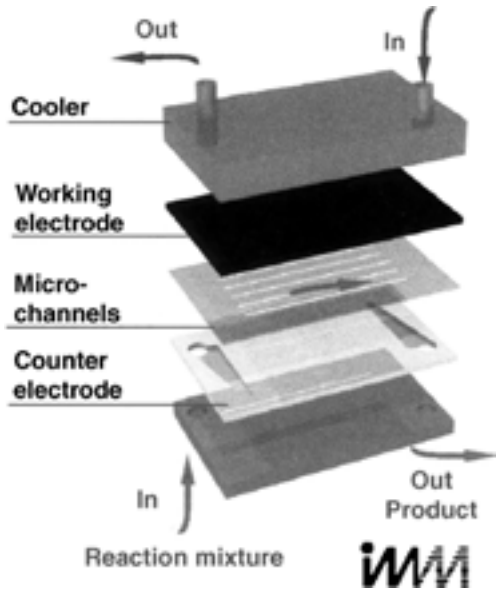

Fig. 4. Schematic representation of assembly of the prototype electrochemical microreactor (source: IMM Mainz, Germany).

reactor design is based on the thin-layer-cell-technique [18] and employs a miniaturized plate-to-plate electrode configuration with a non-conducting housing (Figure 4). The reaction volume consists of several parallel channels in a foil, which are realized by wet etching and laser cutting techniques. The stack construction leads to a modular and compact design, which can easily be adjusted to different reaction systems. For example the electrode distance can be varied by changing the thickness of the foil. Another design alternative is the construction of a divided cell by introducing a membrane between two separate foils containing reaction channels. The stack construction makes it easy to test different materials for electrodes, foils and membranes.

Owing to the advantages of microreaction technology, the reactor can provide increased reaction yields, short residence times and fast dynamics [10].

Recently, a new prototype has been constructed, which fulfils the requirements for the implementation in an electrochemical SMB-process such as pressure tightness and solvent stability [19].

4. Reaction system

The direct electrochemical production of D-arabinose from sodium D-gluconate in water is used as a model system. This reaction has been studied previously by several authors [20–24]. It is of special interest, as it is a representative for the different oxidations in carbohydrate electrochemistry [25] and D-arabinose itself can be used as a precursor for chiral compounds in the pharmaceutical industry, e.g., vitamins [26]. The main reaction is a partial oxidation of gluconate taking place at the anode, given here for the case of an alkaline medium

$$\underset{\text{Gluconate}}{C_6H_{11}O_7^-} + OH^- \longrightarrow \underset{\text{Arabinose}}{C_5H_{10}O_5} + CO_2 + H_2O + 2e^- \tag{2}$$

There are two types of anode side reactions [20–24]. The first is the further oxidation of the pentose arabinose to lower order sugars (such as the four carbon molecule erythrose) or even the complete oxiditation to carbon dioxide. For the first case this can formally be written as

$$\underset{\text{Arabinose}}{C_5H_{10}O_5} + 4OH^- \rightarrow \underset{\text{Erythrose}}{C_4H_8O_4} + CO_2 + 3H_2O + 4e^- \tag{3}$$

The other side reaction is the solvent decomposition of water to oxygen

$$4OH^- \rightarrow 2H_2O + O_2 + 4e^- \tag{4}$$

In the present study, the anode and the cathode compartment of the electrochemical microreactor are separated by an ion exchange membrane so that the hydrogen from the cathode reaction

$$2H_2O + 2e^- \rightarrow H_2 + 2OH^- \tag{5}$$

does not directly interfere with the anode reactions.

5. Mathematical model

5.1. *Electrochemical microreactor*

To perform case studies of the integrated process for a wide range of parameters, it is necessary to ensure sufficiently fast process simulation. Therefore the model of a plug flow reactor with convective mass transport and first order reactions is chosen, which is able to sufficiently reproduce the system behaviour while still guaranteeing fast simulation. Only the reactions in the anode compartment are considered and no electrodynamics are included in this model at present. As the processes at the cathode are assumed to have no direct influence on the reactor performance, these are neglected in the further course of this study. The differential mass balance for each component j is written:

$$\frac{\partial c_j(z,t)}{\partial t} = -u\frac{\partial c_j(z,t)}{\partial z} + R_j \tag{6}$$

with the internal velocity u inside the anode compartment given as

$$u = \frac{\dot{V}}{sbN} \tag{7}$$

It will be shown in the following sections (see Figure 5) that the reaction system can be described with

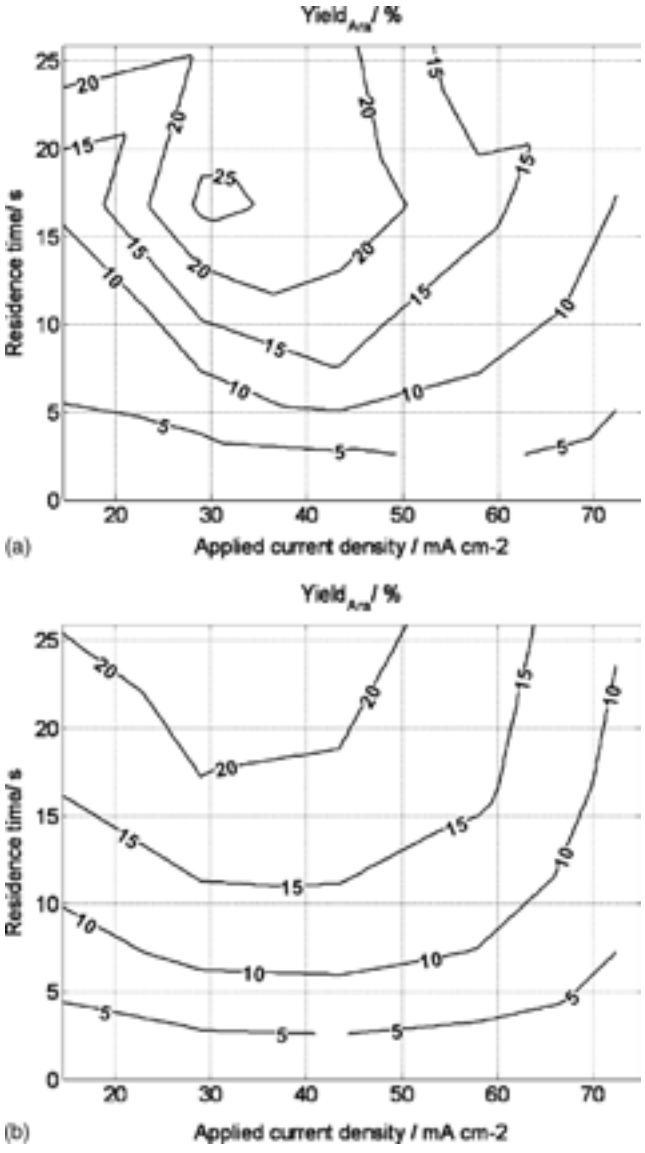

Fig. 5. Comparison of experiment (a) and simulation (b) for the yield of arabinose.

reasonable accuracy as a series reaction: the main reaction is the production of gluconate according to Equation 2, characterized by the rate constant k_1, and the side reaction is the further decomposition of arabinose characterized by the rate constant k_2 (Equation 3):

$$\underset{\text{Gluconate}}{C_6H_{11}O_7^-} \xrightarrow[-n_{eR1}]{k_1(i)} \underset{\text{Arabinose}}{C_5H_{10}O_5} \xrightarrow[-n_{eR2}]{k_2(i)} \underset{\text{Erythrose}}{C_4H_8O_4} \tag{8}$$

Erythrose has been selected as key component for the by-products. Because the rate constants are taken as functions of the applied current density i, the loss of electrical current due to the side reaction of oxygen evolution has been lumped into the rate constants.

Assuming first order reactions, this leads to the following reaction terms R_j for each component (j = Gluc, Ara, Ery):

$$R_{\text{Gluc}} = -k_1(i)c_{\text{Gluc}} \tag{9}$$

$$R_{\text{Ara}} = k_1(i)c_{\text{Gluc}} - k_2c_{\text{Ara}}(i) \tag{10}$$

$$R_{\text{Ery}} = k_2c_{\text{Ara}}(i) \tag{11}$$

Through Faraday's law the reaction rates are linked to the current densities i_{R1} and i_{R2} for each electrochemical reaction:

$$R_{\text{Gluc}} = -\frac{a_e}{n_{eR1}F}i_{R1} \tag{12}$$

$$R_{\text{Ara}} = \frac{a_e}{n_{eR1}F}i_{R1} - \frac{a_e}{n_{eR2}F}i_{R2} \tag{13}$$

$$R_{\text{Ery}} = \frac{a_e}{n_{eR2}F}i_{R2} \tag{14}$$

The resulting linear relationship between current density (Equations 12–14) and concentration (Equations 9–11) is an analytical solution generally derived for diffusion limited reaction conditions, but the simplicity and satisfactory accuracy of the resulting model justifies the assumption of first order reactions in this study.

5.2. *Chromatographic separation process*

In the strategy commonly used, only one column has to be characterized to model an SMB unit as a combination of several columns with periodic changes in the boundary conditions of each column. The theoretical model for a chromatographic column is based on the differential mass balance taking into account axial dispersion as well as mass transfer between fluid and solid phase given by a linear-driving-force (LDF)-model. This leads to the following differential equation for the mass balance of component j (j = Gluc, Ara, Ery) in each section k (k = I,II,III,IV) for the liquid phase:

$$\frac{\partial c_j}{\partial t} = -\frac{\dot{V}_k}{A_C\varepsilon}\frac{\partial c_j}{\partial x} + D_{\text{ax,C}}\frac{\partial^2 c_j}{\partial x^2} - k_{\text{eff},j}\frac{6}{d_p}\frac{1-\varepsilon}{\varepsilon}(c_j - c_{p,j}) \tag{15}$$

and solid phase:

$$\frac{\partial q_j}{\partial t} = k_{\text{eff},j}\frac{6}{d_p}(c_j - c_{p,j}) \tag{16}$$

The axial dispersion coefficient can be estimated by the equation proposed by Chung and Wen [27]:

$$Bo = \frac{\dot{V}_k d_p}{A_C\varepsilon D_{\text{ax,C}}} \tag{17}$$

$$Bo = \frac{0.2}{\varepsilon} + \frac{0.011}{\varepsilon}(\varepsilon Re_p)^{0.48} \tag{18}$$

$$Re_p = \frac{\rho_{fluid}\dot{V}_k d_p}{A_C \varepsilon \eta_{fluid}} \quad (19)$$

and the adsorption equilibrium is described by the isotherm equation:

$$q_j = f(c_{p,j}) \quad (20)$$

These Equations 15–20 describe the model for each individual column.

In the SMB-process the internal flow rates are related to the external streams by balances of the in- and outlet nodes. A mass balance of each node is also necessary to calculate the concentration at the in- and outlet of each single section:

Desorbent node:

$$\dot{V}_D = \dot{V}_I - \dot{V}_{IV} \quad (21)$$

$$c_{j,D}\dot{V}_D = c_{j,I}^{in}\dot{V}_I - c_{j,IV}^{out}\dot{V}_{IV} \quad (22)$$

Extract draw-off node:

$$\dot{V}_E = \dot{V}_I - \dot{V}_{II} \quad (23)$$

$$c_{j,E} = c_{j,I}^{out} = c_{j,II}^{in} \quad (24)$$

Feed node:

$$\dot{V}_F = \dot{V}_{III} - \dot{V}_{II} \quad (25)$$

$$c_{j,F}\dot{V}_F = c_{j,III}^{in}\dot{V}_{III} - c_{j,II}^{out}\dot{V}_{II} \quad (26)$$

Raffinate draw-off node:

$$\dot{V}_R = \dot{V}_{III} - \dot{V}_{IV} \quad (27)$$

$$c_{j,R} = c_{j,III}^{out} = c_{j,IV}^{in} \quad (28)$$

6. Experimental

6.1. *Electrochemical microreactor*

Steady state experiments in the first prototype of the microreactor have been conducted at ambient temperature to determine the reactor performance. The reactor is a divided cell equipped with a proton conducting polyether-etherketone(PEEK)-membrane [28]. All dimensions of the microreactor are given in Table 1.

All reagents were synthesis grade and were purchased from Merck (Darmstadt, Germany). Demineralised water was obtained through a Milli-Q system from Millipore (Bedford, USA). Two pumps L6200A from Merck (Darmstadt, Germay) were used to set the flow rates.

Table 1. Dimensions of the microreactor prototype used for parameter determination (The anode and cathode compartment are of equal size)

Characteristic	Symbol	Value
Distance electrode/membrane	s/μm	125
Membrane thickness	s_m/μm	125
Width of the channel	b/μm	800
Length of the channel	L/cm	3.2
Number of channels	N (–)	27
Volume anode compartment	V_A (μl)	86.4
Electrode surface area	A_e (cm^2)	6.9
Surface to volume ratio (anode)	a_e (cm^{-1})	80

The feed to the anode compartment consisted of 0.5 m sodium gluconate in aqueous solution of 0.5 m sodium acetate, which was used as conducting salt. The feed to the cathode compartment had the same composition but no gluconate was used. Equal flow rates for both compartments were used and their value was varied between 0.2 and 2 ml min^{-1} corresponding to a residence time of the solution in the reaction channels between approx. 26 and 2.6 s, respectively. For each residence time the applied current was varied between 100 and 500 mA, which correspond to current densities of approx. 14.5 to 72.3 mA cm^{-2}.

The solution of arabinose and gluconate leaving the reactor was analyzed by gas chromatography coupled with mass spectroscopy [29]. A Hewlett Packard 5890 Series II gas chromatograph equipped with a standard column (HP5) and a FID detector was used. Product derivatization was performed with hexamethyldisilazane (HMDS, Fluka, p.a.) and trichloromethylsilane (TMCS, Fluka, purum) in aqueous pyridine (Fluka, p.a.) solution.

This procedure allows determination of the conversion of gluconate and the yield of arabinose individually. In Figure 5(a) the experimental result for the yield of arabinose is given.

6.2. *Chromatographic column*

A consistent and experimentally verified method is applied to characterize the chromatographic separation by single column experiments. A detailed description of this method is given elsewhere [30].

The ion exchange resign PCR-450Na (d_p = 380 μm, Purolite) was used as adsorbent. No ion exchange has to be taken into account as the adsorption mechanism in the case of sugars is purely adsorptive. The chromatographic parameters for arabinose (for microbiology, Merck, Germany) and gluconate (synthesis grade, Merck, Germany) in pure water and aqueous solution of 0.5 M sodium acetate (synthesis grade, Merck, Germany) were determined. Apart from adsorption isotherms, the packed bed void fraction and mass transfer coefficients were obtained in a test column of 12 cm length and an inner diameter of 2.6 cm (Superformance, Merck, Germany). A standard LC setup consisting of one pump (Prep Star Solvent delivery Modul SD1, Varian, Germany), a six-port injection

valve (Rheodyne 7125, Rheodyne, USA), a polarimeter detector (IBZ Messtechnik, Germany) and a standard PC was used.

7. Parameter determination

7.1. *Electrochemical microreactor*

For steady state operation, Equation 6 in combination with Equations 9–11 can be solved analytically under the boundary condition that only gluconate is present in the feed stream

$$c_{\mathrm{Gluc}}(z=0)=c_0, \quad c_{\mathrm{Ara}}(z=0)=c_{\mathrm{Ery}}(z=0)=0 \tag{29}$$

This solution can be rewritten to give the following expressions for the conversion of gluconate

$$\mathrm{Con}_{\mathrm{Gluc}}=\frac{c_0-c(z=L)}{c_0}=1-\exp\{-k_1(i)\tau\} \tag{30}$$

and the yield of arabinose at the reactor exit ($z = L$)

$$Y_{\mathrm{Ara}}=\frac{c_{\mathrm{Ara}}(z=L)}{c_0}=\frac{k_1(i)}{k_2(i)-k_1(i)}[\exp\{-k_1(i)\tau\}-\exp\{-k_2(i)\tau\}] \tag{31}$$

The residence time τ is defined as:

$$\tau=\frac{L}{u} \tag{32}$$

The rate constants $k_1(i)$ and $k_2(i)$ are determined for each applied current density by fitting the values of conversion and yield for the experiments with different residence times (Figure 5(a)). This leads to the following empirical correlations:

$$k_1(i)=-1.296\times10^{-5}i^2+1.058\times10^{-3}i \tag{33}$$

$$k_2(i)=1.602\times10^{-5}i^2+1.920\times10^{-3}i \tag{34}$$

Within the parameter range investigated here, the rate constant k_2 is always larger than k_1 by a factor of 1.6–5.2.

The simulation of Equation 6 together with correlations 33 and 34 leads to Figure 5(b). The comparison with Figure 5(a) shows reasonable agreement between experiment and simulation and justifies the use of this model in further process investigations. The developed reaction model is able to reproduce the maximum in the yield as a function of the residence time.

7.2. *Chromatographic column*

Although the isotherm for gluconate was slightly nonlinear, for the sake of simplicity and to eliminate the influence of nonidealities in adsorption behaviour, all isotherms are taken to be linear and are described by Henry coefficients H_j. Equation 20 is thus replaced by

$$q_j=H_jc_{\mathrm{p},j} \tag{35}$$

The Henry coefficients of gluconate and arabinose have been determined as 0.3 and 0.6, respectively. For erythrose the Henry coefficient is arbitrarily set to 0.2 for this study. It is important to state that the value of the Henry coefficient of erythrose relative to those for arabinose and gluconate determines the process set-up: e.g. it is impossible to separate pure arabinose from the reaction mixture in one SMB for a Henry coefficient of erythrose greater than those of arabinose. In this case the design problem becomes much more complex. Although the selection of 0.2 as Henry coefficient is clearly a constraint in terms of process selection, this value makes it easier to demonstrate the performance of the integrated process.

All chromatographic parameters used for this study are summarized in Table 2.

8. Description of the integrated process

The matching operating conditions allow the combination of the electrochemical microreactor and the chromatographic separation process without changing the solvent or the operating temperature. In this study only continuous process operation will be considered, thus limiting the use of chromatography to SMB-operation. If arabinose is to be produced with a purity of 99% in one process step, the yield of the serial connection between reactor and SMB-process is limited by reaction kinetics (Equations 8 and 31) in single pass operation. The arabinose produced during the reaction is partially consumed by further decomposition inside the reactor and is then purified in a SMB unit.

In an integrated process, the microreactors are placed between the chromatographic columns in a standard SMB-set-up (Figure 6).

To overcome the limitation in yield by the continuous removal of arabinose from the reaction zone, the process is operated in the following way (Figure 6(a)): Pure gluconate solution is used as feed in the electrochemical SMB-reactor and the switching of the inlet and outlet ports can be carried out as described above. Arabinose is separated from the reaction mixture and collected at

Table 2. Chromatographic parameters used for process simulation

Characteristic	Symbol	Value
Arabinose/Gluconate/Erythrose		
Henry constant	H (–)	0.6/0.3/0.2
Mass transfer coefficient	k_{eff} ($\times10^{-4}$ cm s^{-1})	3.5/1.7/3.5
Adsorbent		
Particle diameter	d_{p} (cm)	0.038
Void fraction	ε (–)	0.3218

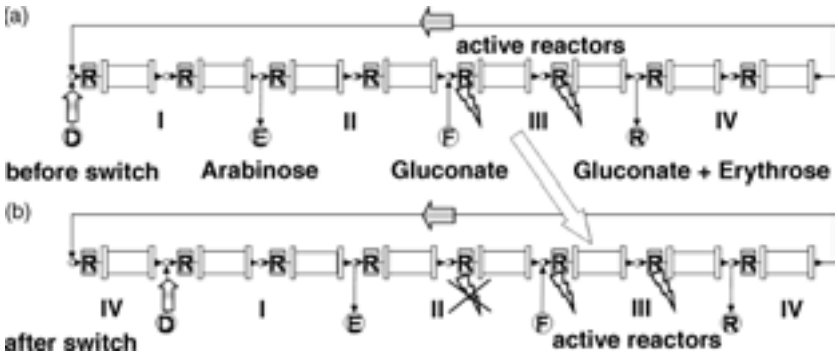

Fig. 6. (a,b) Operating principle of the electrochemical SMB-reactor for the production of arabinose.

the extract port. The raffinate contains unreacted gluconate and the by-product erythrose. This makes a direct recycle of gluconate impossible, as erythrose would accumulate in the process. A purge has to be included in the recycle to avoid this problem, which goes beyond the scope of this paper.

As gluconate is mainly present in zone III, the reaction should only take place in this section of the process. Therefore only the reactors in this section need to be active and are switched on. Additionally, it is important that the other reactors are inactive to avoid arabinose and solvent decomposition.

A switch of the inlet and outlet ports of the SMB-process (Figure 6(b)) also has to include a shift of the active reactors. This is only possible because electrochemical reactions exhibit the unique feature to be switched on and off by means of the applied current. During the shift one reactor is switched on and the other is switched off. Another important point is the necessity to use microreactors in this process to achieve fast fluid and electrical dynamics in the reactors. Otherwise the discontinuous reactor operation would likely lead to instabilities in the process.

In Figure 7 the concentration profile inside the SMB-reactor obtained from simulation is given. The inlet concentration of gluconate into the second active reactor is higher than the outlet concentration of the first one while the opposite is true for arabinose. This clearly demonstrates the interaction of reaction and separation in this integrated process.

9. Model based process synthesis: Case studies

Because of the complex behaviour of this periodic process, a model-based approach for the process layout and design is necessary. Based on the units 'reactor' and 'column', two different processes have been investigated. A serial design with an electrochemical reactor followed by a SMB-separation and an integrated process with reactors placed between the columns of the SMB-process as described above. The process models have been implemented in the dynamic simulation program gPROMS™ (Process Systems Enterprise Limited).

A conventional set-up of the SMB-process consisting of eight columns with two columns per section is considered. In the integrated case only the two reactors in zone III are active. In the serial case two reactors are placed in front of the SMB, so that the total active reactor volume is the same for both processes (Figure 8).

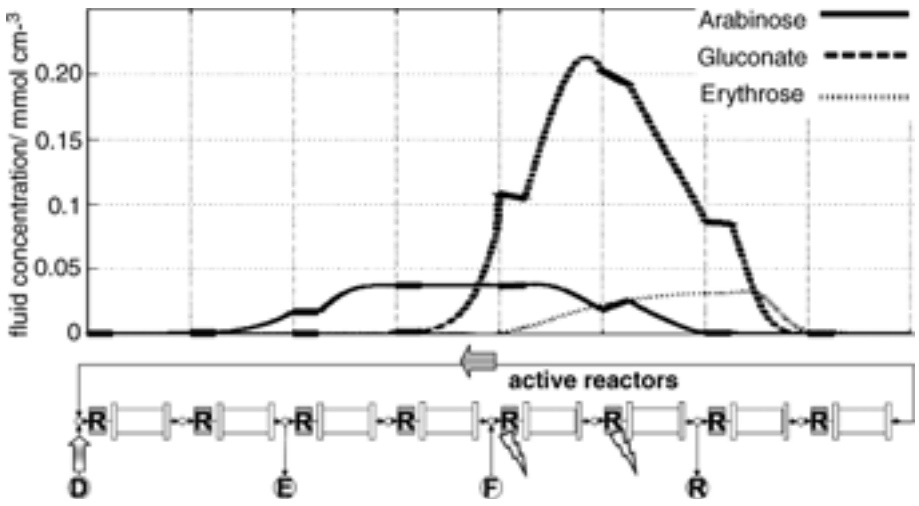

Fig. 7. Simulated internal concentration profile in a SMB-reactor for the production of arabinose ($m_{II} = 0.35$, $m_{III} = 0.354$, other data taken from Table 3).

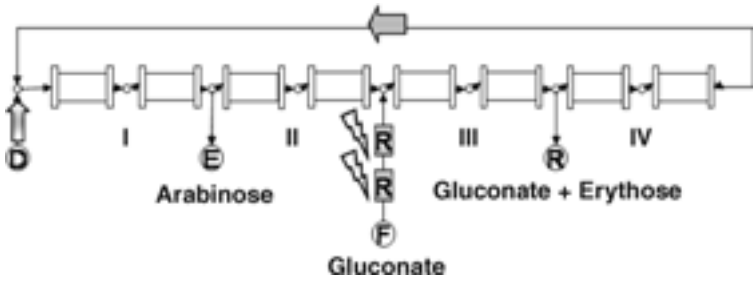

Fig. 8. Process description for the serial (R + SMB) connection of reactor and SMB.

Table 3. Input parameters used in the case studies

Reactor		SMB[a]	
L (cm)	20	L_C (cm)	60
s (μm)	125	A_C (cm^2)	5.31
b (μm)	800	ρ_{fluid} (g cm^{-3})	1
N (–)	71	η_{fluid} (g cm^{-1} s^{-1})	10^{-3}
k_1 (s^{-1})	0.021478	m_I; m_{IV} (–)	0.659; 0.15
k_2 (s^{-1})	0.053139	t_{switch} (s)	306
n_R (–)	2	n_C (per section)	8 (2)

[a] Other data taken from Table 2.

The parameters used in this study are summarized in Table 3.

The dimensionless flow rates m_k in zone II and III, defined for SMB as

$$m_k = \frac{\dot{V}_k t_{switch} - A_C L_C \varepsilon}{A_C L_C (1-\varepsilon)} \tag{36}$$

are varied systematically. The interval for the parameters are selected according to the Henry coefficients of the species, as suggested by the equilibrium theory [11–13]. The influence of the operating parameters on the overall yield of arabinose in the extract over one cycle,

$$Y_{Ara,E} = \frac{\dot{n}_{Ara,E}}{\dot{V}_F c_{Gluc,F}} \tag{37}$$

and the productivity or space time yield of arabinose based on the total reactor volume

$$Pr_{Ara,E} = \frac{\dot{n}_{Ara,E}}{sbNLn_R} \tag{38}$$

is studied. The amount of arabinose collected at the extract port during one cycle can be calculated by applying the following equation in cyclic steady state:

$$\dot{n}_{Ara,E} = \frac{\dot{V}_E}{n_C t_{switch}} \int_0^{n_C \cdot t_{switch}} c_{Ara,E}(t)\mathrm{d}t \tag{39}$$

The purity in the extract is calculated by the following equation:

$$Pur_{Ara,E} = \frac{\dot{n}_{Ara,E}}{\dot{n}_{Ara,E} + \dot{n}_{Gluc,E} + \dot{n}_{Ery,E}} \tag{40}$$

The results from simulation for the integrated process are given in Figure 9. The yield of arabinose (Figure 9(a)) exhibits a maximum of 60% for m_{II} about 0.32 and m_{III} about 0.325.

This corresponds to a region of low feed flow rates, because m_{III}–m_{II} is proportional to the feed, as can be seen by combining Equations 25 and 36:

$$m_{III} - m_{II} = (\dot{V}_{III} - \dot{V}_{II}) \frac{t_{switch}}{L_C A_C (1-\varepsilon)} = \dot{V}_F \frac{t_{switch}}{L_C A_C (1-\varepsilon)} \tag{41}$$

However, if taking into account the purity constraint of 99% (given as lines of constant purity in Figure 9), the operating range of the process is limited to flow rates m_{II} greater 0.345. This lowers the maximum achievable yield to only 48%. As shown in the figure, a less strict purity specification of e.g. 90% would allow operation with much higher yields of about 59%.

Although further optimization of e.g. the reactor and column volumes might produce higher reaction yields, the series reaction inside the reactor limits the maximum yield to well below 100% for still reasonable conversion of gluconate.

The productivity as a function of the operating parameters shows a trend opposite to that one for the yield (Figure 9(b)). It reaches a maximum in regions of low m_{II} and high m_{III}. Although the yield is low in these regions, the high feed throughput leads to a higher amount of product and, therefore, higher productivity. In terms of process optimization, it is important to define the desired objective function in order to select optimal process conditions. In general this will be a cost function, which in the case studied here could be generated by properly weighing yield and productivity with specific costs. However, for identifying general trends in process behaviour, this is not necessary.

The importance of selecting a proper objective function can also be shown by a comparison of the integrated process (SMBR) and the serial connection of reactor and SMB-separation (R + SMB) (Figure 10). The purity in the extract was always greater 99% for both processes.

The integrated process can produce arabinose with significantly higher yield than the serial process, which is limited by the maximum yield typical for a series

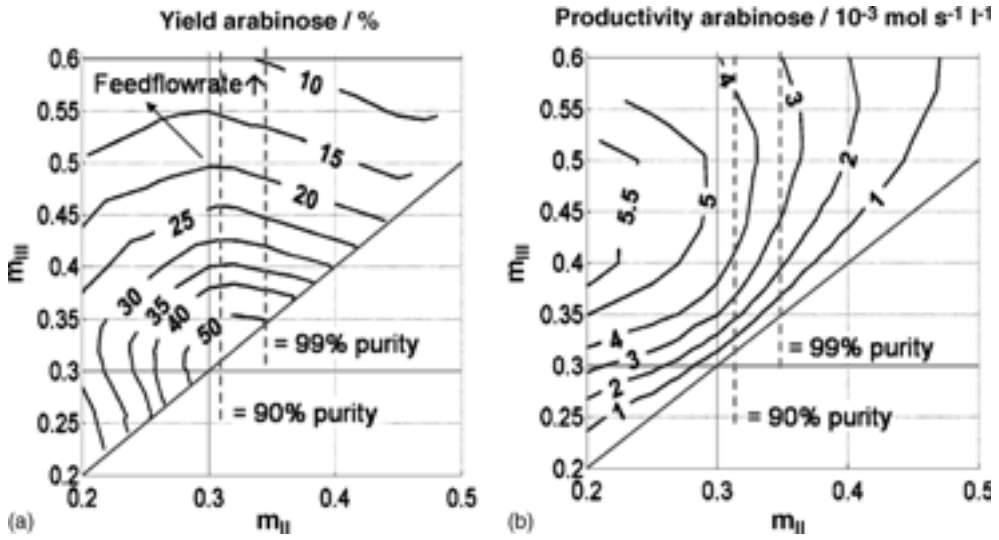

Fig. 9. Influence of operating parameters on the (a) yield and (b) productivity of arabinose in the extract obtained from simulation ((- - -) line of constant purity).

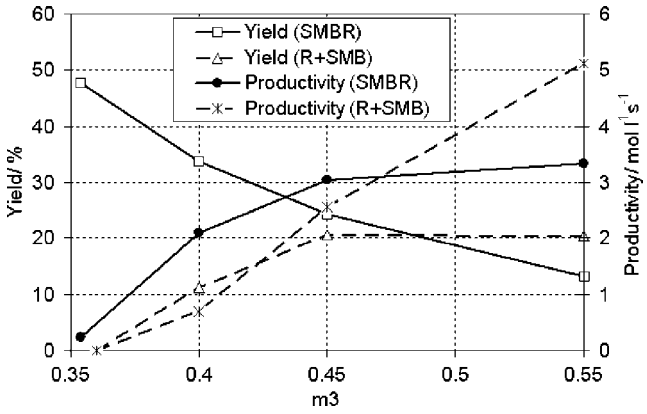

Fig. 10. Comparison of integrated (SMBR) and serial (R + SMB) connection of reactor and SMB: yield and productivity of arabinose in the extract ($m_{II} = 0.35$; extract purity >99%; theoretical maximum yield for serial connection: 21.9%).

reaction. This can be seen from Figure 10, where the maximum yield for the latter case is very close to the theoretical limit of 21.9%. But the simulation data also indicate that the maximum productivity in the latter case can be higher than in the integrated case.

Therefore it is not a priori clear if the integrated process is 'better' than the serial connection.

10. Conclusion

Electrochemical SMB-reactors integrate electrochemical microreactors and chromatographic separation columns in a countercurrent simulated moving bed process. Different operation modes of this process are presented to demonstrate the potential for process intensification by process integration.

A model based simulation strategy has been used to examine the application of this process to the direct electrochemical production of arabinose. It has been shown that the microreactor can be described by a simple plug-flow model with a series reaction. Together with the experimentally verified model of the chromatographic column, the whole process can be described.

To integrate the reaction in an SMB-process, the electrochemical microreactors are placed between the columns and the system is operated in SMB-mode. For arabinose production, the reactors should be active in the zone with the highest gluconate concentration. In addition to the matching operating conditions, this shows the advantage of connecting electrochemical reactors and SMB, as the reactors can be switched 'on' and 'off' by means of the applied current. Microreactors are necessary to achieve fast process dynamics. The case studies performed prove the feasibility of the integrated process, as higher yields than with a serial connection of reactor and SMB can be obtained. Appropriate objective functions for process optimization are also discussed: The integrated process will obtain high productivity only at low yield and vice versa. A comparison of integrated and serial operating processes leads to similar results. Whereas a higher maximum yield can be obtained in the integrated case, the serial case seems to achieve a higher maximum productivity.

More case studies must to be performed and suitable objective functions have to be taken into account to compare these two processes on a broader basis, which should also include the variation of design parameters and the recycle of unused reagents.

Acknowledgements

Funding from the German Federal Ministry of Education and Research (BMBF) through grant no. 03C0327 is gratefully acknowledged.

References

1. R. Krishna, *Chem. Eng. Sci.* **57** (2002) 1491.
2. R. Ditz, M. Schulte and J. Strube, *Curr. Opin. Drug. Discovery Develop.* **1** (1998) 264.
3. M. Schulte and J. Strube, *J. Chromatogr. A* **906** (2001) 399.
4. S.H. Langer and J.E. Patton, *in* J.H. Purnell (Ed.), 'New Developments in Gas Chromatography' (Wiley-Interscience, 1973) p. 293.
5. J. Fricke, H. Schmidt-Traub and M. Kawase, *in* 'Ullmann's Encyclopedia of Industrial Chemistry' (WILEY-VCH, 6th edn., 2000).
6. F. Lode, M. Houmard, C. Migliorini, M. Mazzotti and M. Morbidelli, *Chem. Eng. Science* **56** (2001) 269.
7. R.W. Carr and H. Dandekar, *in* S. Kulprathipanja (Ed.), 'Reaction Separation Processes' (Taylor & Francis, New York, 2002), pp. 115–154.
8. H. Loewe, M. Kuepper and A. Ziogas, *German patent DE 19841302A1*, *European patent EP* 99/06684.
9. H. Loewe, M. Kuepper and A. Ziogas, *in* W. Ehrfeld (Ed.), 'Microreaction Technology: Industrial Prospects', Proceeding of the third International Conference on Microreaction Technology (IMRET3), (Springer-Verlag, Berlin, 2000), p. 126–136.
10. W. Ehrfeld, V. Hessel and H. Löwe, 'Microreactors – New Technologies for Modern Chemistry' (WILEY-VCH, 1st edn. 2000).
11. D.M. Ruthven and C.B. Ching, *Chem. Eng. Sci.* **44** (1989) 1011.
12. F. Charton and R.M. Nicoud, *J. Chromatogr. A* **702** (1995) 97.
13. M. Mazotti, G. Storti and M. Morbidelli, *J. Chromatogr.* **769** (1997) 3.
14. D.B. Broughton, *US patent 2.985.589* (1961).
15. G. Ganetsos and P.E. Barker (Eds), *Preparative and Production Scale Chromatography* (Marcel Dekker, New York 1993).
16. D.B. Broughton, *Chem. Eng. Prog.* **64** (1968) 60.
17. D.B. Broughton, H.J. Bieser, R.C. Berg and E.D. Conell, *Suc. Belg.* **96** (1977) 155.
18. F.E. Woodard and C.N. Reilley, *in* V. Yeager, J.O.M. Bockris, P.P. Conway and S.T. Sarangbani (Eds), 'Comprehensive. Treatise of Electrochemistry' Vol. 9 (Plenum Press, New York, 1984), pp. 353–392.
19. M. Küpper, V. Hessel and H. Löwe, *Electrochim. Acta* (in press).
20. V. Jiricny and V. Stanek, *J. Appl. Electrochem* **24** (1994) 930.
21. V. Jiricny and V. Stanek, *Collect. Czech. Chem. Commun.* **60** (1995) 863.
22. G. Pezzatini, H. Wie, R. Guidelli and F. Pergola, *Electroanalysis* **4** (1992) 129.
23. F. Pergola, L. Nucci, G. Pezzatini, H. Wie and R. Guidelli, *Electrochim. Acta* **39** (1995) 1415.
24. C. Vallieres and M. Matlosz, *J. Electrochem. Soc.* **146** (1999) 2933.
25. M. Baizer and H. Lund (Eds), *Organic Electrochemistry* (Marcel Dekker, New York, 1983).
26. W. Dobler, H. Ernst and J. Paus, *German patent DE 3622643 A1* (1988).
27. S.F. Chung and C.Y. Wen, *AIChE J.* **14**, No. 6 (1968) 857.
28. M. Küpper, V. Hessel and H. Löwe, Proceedings of the 53rd Annual Meeting of the International Society of Electrochemistry (Düsseldorf, Germany, 15–20 September 2002), p. 238.
29. I. Molnar-Perl, *J. Chromatogr. A* **891** (2000) 1.
30. U. Altenhöner, M. Meurer, J. Strube and H. Schmidt-Traub, *J. Chromatogr. A* **769** (1997) 59.